# Ligand Design for Alkali-Metal-Templated Self-Assembly of Unique High-Nuclearity $Cu^{II}$ Aggregates with Diverse Coordination Cage Units: Crystal Structures and Properties

**Miao Du,[a] Xian-He Bu,*[a] Ya-Mei Guo,[a] and Joan Ribas[b]**

**Abstract:** The construction of two unique, high-nuclearity $Cu^{II}$ supramolecular aggregates with tetrahedral or octahedral cage units, $\{(\mu_3\text{-Cl})[Li\subset Cu_4(\mu\text{-}L^1)_3]_3\}(ClO_4)_8(H_2O)_{4.5}$ (**1**) and $\{[Na_2\subset Cu_{12}(\mu\text{-}L^2)_8(\mu\text{-Cl})_4](ClO_4)_8(H_2O)_{10}(H_3O^+)_2\}_\infty$ (**2**) by alkali-metal-templated ($Li^+$ or $Na^+$) self-assembly, was achieved by the use of two newly designed carboxylic-functionalized diazamesocyclic ligands, *N*,*N*′-bis(3-propionyloxy)-1,4-diazacycloheptane ($H_2L^1$) or 1,5-diazacyclooctane-*N*,*N*′-diacetate acid ($H_2L^2$). Complex **1** crystallizes in the trigonal $R\bar{3}c$ space group ($a = b = 20.866(3)$, $c = 126.26(4)$ Å and $Z = 12$), and **2** in the triclinic $P\bar{1}$ space group ($a = 13.632(4)$, $b = 14.754(4)$, $c = 19.517(6)$ Å, $\alpha = 99.836(6)$, $\beta = 95.793(5)$, $\gamma = 116.124(5)°$ and $Z = 1$). By subtle variation of the ligand structures and the alkali-metal templates, different polymeric motifs were obtained: a dodecanuclear architecture **1** consisting of three $Cu_4$ tetrahedral cage units with a $Li^+$ template, and a supramolecular chain **2** consisting of two crystallographically nonequivalent octahedral $Cu_6$ polyhedra with a $Na^+$ template. The effects of ligand functionality and alkali metal template ions on the self-assembly processes of both coordination supramolecular aggregates, and their magnetic behaviors are discussed in detail.

**Keywords:** alkali metals · coordination polyhedra · copper · template synthesis

## Introduction

The self-assembly of high-nuclearity metal-organic aggregates, especially for paramagnetic polyhedral cage complexes, has become a focus in recent years on account of the fascinating structures of these compounds and their importance in host–guest chemistry associated with suitable central cavities. These aggregates also have other potential applications.[1] A variety of organic bridging spacers involving carboxylate or alkoxide,[2] multidendate heterocycles,[3] phosphonate or phosphinate,[4] and other spacers[5] have been employed for the design of these aggregates, and a series of coordination cages, termed Platonic solids (e.g., tetrahedron, cube, octahedron, dodecahedron, and icosahedron) or Archimedean solids (e.g. truncated tetrahedron, cuboctahedron, truncated cube, and snub cube), in addition to other types of solids (e.g. trigonal bipyramid, adamantanoid, and trigonal prism) have been constructed by self-assembly by the use of the aforementioned ligands.[1h] In addition, the smallest cage unit, the tetrahedral system, has attracted much interest since it was discovered that it is also the smallest aggregate showing single molecule magnet (SMM) behavior.[6] Furthermore, the counteranions, such as halide, perchlorate, or tetrafluoroborate, commonly act as templates in the construction of the polymetallic cages.[2–5] However, templated cage formation with cations, such as an alkali metal or $R_4N^+$, is still rather limited.[7]

As described by us[8,9] and others,[10] diazamesocycles, especially 1,5-diazacyclooctane (DACO), modified by suitable donor pendants, can be used as building blocks to construct polymeric systems with unique structures and properties. Recently, we attempted to incorporate the carboxylic group, a versatile group displaying a variety of coordination modes, onto the backbone of DACO. In this process, some fascinating chemistry of this ligand ($H_2L$) was observed under self-assembly conditions with metal ions.[9] One of the main reasons justifying the continuous interest in this attractive system is the construction of other novel metal-organic architectures with special topologies and properties by modifying the backbone of the diazamesocycle, for example, by choosing 1,4-diazacycloheptane (DACH) as the initial material, or by altering the functional pendant arm on DACO.

[a] Dr. M. Du, Prof. X.-H. Bu, Y.-M. Guo
Department of Chemistry, Nankai University
Tianjin 300071 (China)
Fax: +(86) 22-23502458
E-mail: buxh@nankai.edu.cn

[b] Prof. J. Ribas
Department de Química Inorgànica, Universitat de Barcelona
08028 Barcelona (Spain)

Supporting information for this article is available on the WWW under http://www.chemeurj.org/ or from the author.

 **DOI: 10.1002/chem.200305300**  

Herein, we report the preparation, crystal structures, and magnetic behaviors of two remarkable high-nuclearity supramolecular $Cu^{II}$ aggregates formed by alkali-metal-templated self-assembly of $[Cu(ClO_4)_2]$ and two well-designed ligands, *N*,*N*′-bis(3-propionyloxy)-1,4-diazacycloheptane ($H_2L^1$) and 1,5-diaza-cyclooctane-*N*,*N*′-diacetate acid ($H_2L^2$, Scheme 1).

## Results and Discussion

**Comments on the crystal structures of complexes 1 and 2**: The X-ray crystal structure of **1** shows that it has a dodecanuclear architecture in which three tetrahedral $Cu_4$ aggregates are linked through an unusual $\mu_3$-Cl bridge. They are related to each other by a threefold symmetry axis that passes through the chloride center. Four crystallographically independent $Cu^{II}$ centers bridged by six carboxylic groups in $\mu$-$O_{syn}$,$O'_{anti}$ mode (Scheme 2a) result in a tetrahedral $Cu_4$ motif (Figure 1). Selected bond lengths and angles for structure **1** are given in Table 1. Cu1, Cu2, and Cu3 have similar distorted square-pyramidal ($CuN_2O_3$) coordination spheres (structural parameter $\tau$ = 0.038, 0.03, and 0.2, respectively[11]), with two nitrogen atoms and two oxygen donors of the same ligand occupying the basal positions, and an oxygen atom from another adjacent ligand as the apical site. The carboxylic groups and the three $Cu^{II}$ centers form a 12-membered ring (-Cu-O-C-O-)$_3$ consisting of the basal plane

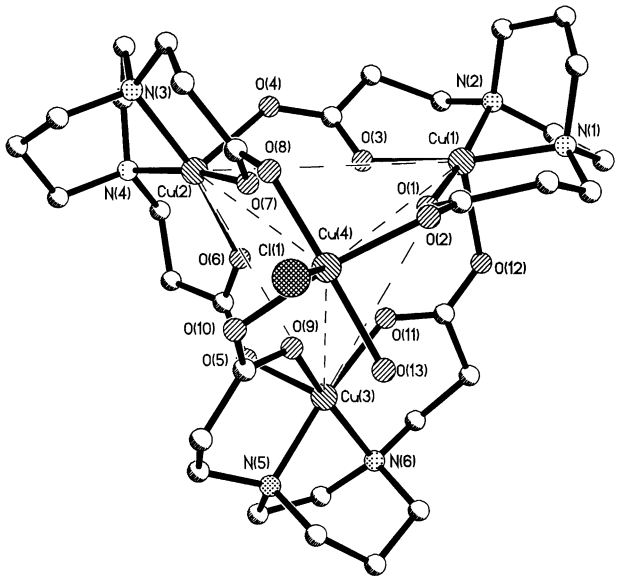


Figure 1. The $Cu_4$ tetrahedral cage unit in the structure of **1**. Bond length ranges [Å]: Cu–O (equatorial sites) 1.928–2.005, Cu–O (axial) 2.183–2.222, Cu–N 1.969–2.010.

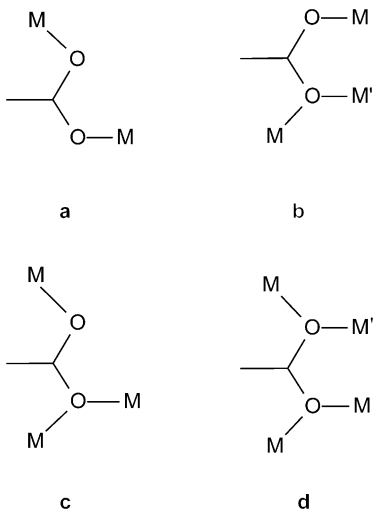


Scheme 2. Bridging modes of the carboxylic groups in **1** and **2**

Table 1. Selected bond lengths [Å] and angles [°] for complex **1**.

| | | | | | |
|---|---|---|---|---|---|
| Cu1–O3 | 1.935(6) | Cu1–N1 | 1.985(8) | Cu1–N2 | 1.996(8) |
| Cu1–O1 | 2.005(6) | Cu1–O12 | 2.222(7) | Cu2–O6 | 1.946(6) |
| Cu2–N3 | 1.969(7) | Cu2–O7 | 1.988(5) | Cu2–N4 | 2.010(7) |
| Cu2–O4 | 2.183(7) | Cu3–O11 | 1.918(6) | Cu3–O9 | 1.968(6) |
| Cu3–N5 | 1.981(7) | Cu3–N6 | 1.999(7) | Cu3–O5 | 2.215(6) |
| Cu4–O8 | 1.928(6) | Cu4–O2 | 1.941(6) | Cu4–O10 | 1.965(6) |
| Cu4–O13 | 2.003(6) | Cu4–Cl1 | 2.644(1) | O3-Cu1-N1 | 170.9(3) |
| O3-Cu1-N2 | 96.0(3) | | | | |
| N1-Cu1-N2 | 80.7(4) | O1-Cu1-O3 | 85.0(2) | O1-Cu1-N1 | 96.6(3) |
| N2-Cu1-O1 | 168.6(3) | O3-Cu1-O12 | 94.1(3) | N12-Cu1-O12 | 94.8(3) |
| N2-Cu1-O12 | 97.9(3) | O1-Cu1-O12 | 93.4(2) | O6-Cu2-N3 | 169.3(3) |
| O6-Cu2-O7 | 84.1(2) | N3-Cu2-O7 | 96.3(3) | O6-Cu2-N4 | 96.3(3) |
| N3-Cu2-N4 | 81.0(3) | O7-Cu2-N4 | 167.5(3) | O6-Cu2-O4 | 95.2(3) |
| O4-Cu2-N3 | 95.2(3) | O7-Cu2-O4 | 99.5(2) | O4-Cu2-N4 | 92.9(3) |
| O11-Cu3-O9 | 85.4(2) | O11-Cu3-N5 | 172.0(3) | O9-Cu3-N5 | 94.2(3) |
| O11-Cu3-N6 | 96.8(3) | O9-Cu3-N6 | 160.0(3) | N5-Cu3-N6 | 80.9(3) |
| O11-Cu3-O5 | 95.5(3) | O9-Cu3-O5 | 100.9(2) | N5-Cu3-O5 | 92.5(3) |
| N6-Cu3-O5 | 98.7(3) | O8-Cu4-O2 | 93.9(3) | O8-Cu4-O10 | 93.1(3) |
| O2-Cu4-O10 | 166.2(3) | O8-Cu4-O13 | 178.4(3) | O2-Cu4-O13 | 87.6(3) |
| O13-Cu4-O10 | 85.3(3) | O8-Cu4-Cl1 | 90.6(2) | O2-Cu4-Cl1 | 101.6(2) |
| O10-Cu4-Cl1 | 90.2(2) | O13-Cu4-Cl1 | 89.7(2) | | |

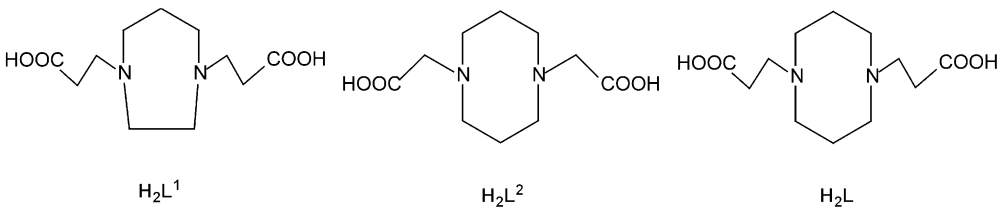


Scheme 1.

of each tetrahedron (Cu···Cu distances within this plane are 5.037, 5.173, and 4.941 Å, respectively). Cu4 is located at the vertex of each tetrahedron, and has a $CuO_4Cl$ geometry ($\tau = 0.203$) with three oxygen donors from different ligands and one aqua ligand in the equatorial sites and one $\mu_3$-Cl as the axis. This atom is separated from other three $Cu^{II}$ centers by 4.976, 4.999, and 4.663 Å, respectively. Cu4 together with any other two $Cu^{II}$ centers also forms a 12-membered ring $(\text{-Cu-O-C-O-})_3$ and represents the side face of each tetrahedron.

It is interesting that in each $Cu_4$ entity there is an encapsulated $Li^+$ ion as the template. It forms electrovalent bonds (bond lengths range from 2.045(15)–2.229(14) Å with average value of 2.127 Å, bond angles in 165.6(8)–169.4(8)° and 75.2(5)–107.6(6)° ranges) with the surrounding six oxygen atoms of the carboxylic pendants. Thus, considering the coordination to both $Cu^{II}$ and $Li^+$, the bridging mode of each carboxylic group is unique $\mu\text{-}O_{Cu(anti)}, O'_{Cu(syn)}\text{-}\mu\text{-}O_{Cu(anti)}, O_{Li(syn)}$ (Scheme 2b). The four Cu···Li separations are 3.000(13), 2.950(14), 3.021(14), and 3.260(14) Å, respectively, and the six Cu-O-Li bridging angles are in the range 90.8(4)–97.8(4)°. The central $\mu_3$-Cl bridges three $Cu_4$ cages with a Cu-Cl-Cu angle of 116.52(5)° to form the overall dodecanuclear architecture (Figure 2) with high symmetry. To our knowledge, this is a new structural type for polynuclear $Cu^{II}$ complexes. The shortest Cu···Cu distance between the $Cu_{12}$ entities is 7.790 Å. Each ligand serves as the chelated agent for one $Cu^{II}$ ion, with the DACH ring adopting the normal boat configuration, and bridges the other two $Cu^{II}$ ions through two pendant arms. In addition, the axial Cu–Cl bond length is rather long (2.644(1) Å), indicating weaker coordination and may be replaced by other stronger field bridging anions, such as $N_3^-$ or $SCN^-$, to form other coordination architectures.

The crystal structure of complex **2** consists of $Cu_6$ entities linked together by asymmetric $Cu(\mu\text{-}O)_2Cu$ bridges to give an infinite one-dimensional (1D) supramolecular system. In this coordination chain there are two crystallographically nonequivalent $Cu_6$ entities with only small structural differences (Figure 3). Selected bond lengths and angles for structure **2** are listed in Table 2. The metal framework in each hexameric unit may be described as a cage with pseudocubic $O_h$ symmetry. In each cage, two chelated $Cu^{II}$ atoms (Cu1 and Cu1A for the right cage, Cu6 and Cu6B for the left cage in Figure 3) and two bridging $Cu^{II}$ atoms (Cu3 and Cu3A for the right cage, and Cu4 and Cu4B for the left cage) are located at the equatorial vertices of a regular nonbonding octahedron. The other two chelated $Cu^{II}$ centers (Cu2 and Cu2A for the right cage, and Cu5 and Cu5B for the left cage) are situated at the axial vertices. In each coordination octahedron, six $Cu^{II}$ centers are bridged by eight carboxylic groups in a $\mu\text{-}O_{syn}, O'_{anti}$ mode (Scheme 2a). Cu1, Cu2, Cu5, and Cu6 have a similar, almost ideal, square-pyramidal ($CuN_2O_2Cl$) coordination sphere (structural parameter $\tau = 0.005$, 0.0, 0.075, and 0.012, respectively[11]), with the two nitrogen atoms and two oxygen donors of the same ligand occupying the basal positions, and a chloride anion at the apical position. The $Cu^{II}$ ions deviate from the mean equatorial plane of the square pyramid toward the axial chloride atom by 0.39, 0.37, 0.37, and 0.39 Å, respectively. It is interesting that two independent chelated $Cu^{II}$ centers within one cage are linked by a single chloro bridge that occupies the apical position, with an average Cu–Cl bond length of 2.483 Å, and a Cu-Cl-Cu angle of 109.66(7) and 108.95(7)°. For the Cu3 and Cu4 centers, five atoms from different carboxylic groups comprise their square-pyramidal coordination with $\tau$ values of 0.015 and 0.017. The $Cu^{II}$ ions

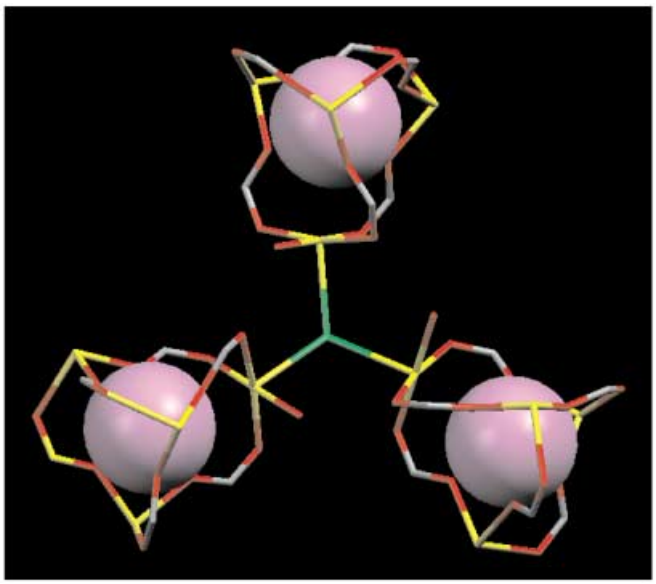

Figure 2. View of the $\{(\mu_3\text{-Cl})[Li\subset Cu_4(\mu\text{-}L_3)]_3\}^{8+}$ ion in **1** (Cu: yellow; Cl: green; O: red; C: gray; $Li^I$ template: purple).

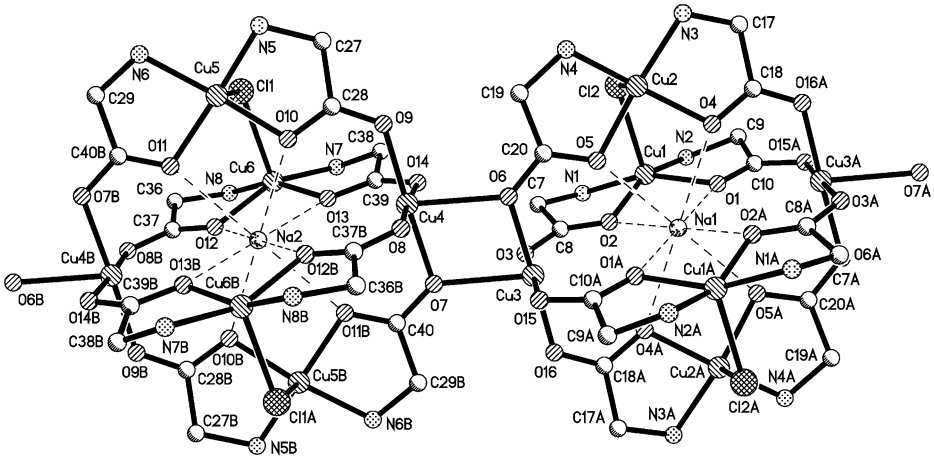


Figure 3. View of the two nonequivalent $Cu_6$ cage units in **2**. The propyl groups on the backbone of DACO and hydrogen atoms were omitted for clarity.

  

Table 2. Selected bond lengths [Å] and angles [°] for complex **2**.

| | | | | | |
|---|---|---|---|---|---|
| Cu1–O1 | 1.956(4) | Cu1–O2 | 1.973(4) | Cu1–N1 | 1.977(5) |
| Cu1–N2 | 1.994(6) | Cu1–Cl2 | 2.489(2) | Cu2–O4 | 1.952(4) |
| Cu2–O5 | 1.977(4) | Cu2–N3 | 1.983(5) | Cu2–N4 | 1.987(6) |
| Cu2–Cl2 | 2.491(2) | Cu3–O16 | 1.921(5) | Cu3–O3 | 1.937(5) |
| Cu3–O6 | 1.964(5) | Cu3–O15 | 1.969(5) | Cu3–O7 | 2.305(4) |
| Cu4–O6 | 2.343(4) | Cu4–O7 | 1.978(5) | Cu4–O8 | 1.953(5) |
| Cu4–O9 | 1.934(5) | Cu4–O14 | 1.923(5) | Cu5–N5 | 1.982(5) |
| Cu5–N6 | 1.992(6) | Cu5–O10 | 1.963(4) | Cu5–O11 | 1.946(4) |
| Cu5–Cl1 | 2.490(2) | Cu6–N7 | 1.980(6) | Cu6–N8 | 1.980(6) |
| Cu6–O12 | 1.983(5) | Cu6–O13 | 1.949(5) | Cu6–Cl1 | 2.463(2) |
| O1-Cu1-O2 | 91.7(2) | O1-Cu1-N1 | 157.4(2) | O2-Cu1-N1 | 84.0(2) |
| O1-Cu1-N2 | 84.8(2) | O2-Cu1-N2 | 157.1(2) | N1-Cu1-N2 | 90.6(2) |
| O1-Cu1-Cl2 | 99.3(2) | O2-Cu1-Cl2 | 95.3(2) | N1-Cu1-Cl2 | 103.2(2) |
| N1-Cu1-Cl2 | 107.6(2) | O4-Cu2-O5 | 91.8(2) | O4-Cu2-N3 | 85.0(2) |
| O5-Cu2-N3 | 158.3(2) | O4-Cu2-N4 | 158.3(2) | O5-Cu2-N4 | 84.4(2) |
| N4-Cu2-N3 | 90.7(2) | O4-Cu2-Cl2 | 96.7(2) | O5-Cu2-Cl2 | 97.7(1) |
| N3-Cu2-Cl2 | 104.0(2) | N4-Cu2-Cl2 | 105.0(2) | O16-Cu3-O3 | 92.2(2) |
| O16-Cu3-O6 | 177.6(2) | O6-Cu3-O3 | 89.4(2) | O16-Cu3-O15 | 88.0(2) |
| O15-Cu3-O3 | 178.5(2) | O15-Cu3-O6 | 90.3(2) | O16-Cu3-O7 | 100.0(2) |
| O3-Cu3-O7 | 84.6(2) | O6-Cu3-O7 | 78.4(2) | O15-Cu3-O7 | 93.9(2) |
| O14-Cu4-O9 | 87.0(2) | O14-Cu4-O8 | 176.8(2) | O8-Cu4-O9 | 94.2(2) |
| O14-Cu4-O7 | 91.8(2) | O7-Cu4-O9 | 177.8(2) | O8-Cu4-O7 | 86.9(2) |
| O6-Cu4-O14 | 87.8(2) | O6-Cu4-O9 | 100.9(2) | O8-Cu4-O6 | 89.1(2) |
| O7-Cu4-O6 | 77.3(2) | O11-Cu5-O10 | 92.4(2) | O11-Cu5-N5 | 160.8(2) |
| O10-Cu5-N5 | 84.3(2) | O11-Cu5-N6 | 84.8(2) | O10-Cu5-N5 | 156.3(2) |
| N5-Cu5-N6 | 90.7(2) | O11-Cu5-Cl1 | 97.8(2) | O10-Cu5-Cl1 | 96.4(2) |
| N5-Cu5-Cl1 | 101.3(2) | N6-Cu5-Cl1 | 107.3(2) | O13-Cu6-N7 | 84.5(2) |
| O13-Cu6-N8 | 157.6(2) | N7-Cu6-N8 | 90.5(3) | O13-Cu6-O12 | 92.3(2) |
| N7-Cu6-O12 | 156.9(2) | O12-Cu6-N8 | 83.8(2) | O13-Cu6-Cl1 | 98.0(2) |
| N7-Cu6-Cl1 | 106.6(2) | Cl1-Cu6-N8 | 104.4(2) | O12-Cu6-Cl1 | 96.4(2) |

deviate from the equatorial coordination plane by only 0.03 and 0.04 Å owing to the lack of the chelate effect of the ligand. In addition, Cu3 and Cu4, which are located at the corner of two different coordination cages, are linked through a pair of carboxylic groups with a Cu···Cu separation of 3.348 Å and Cu-O-Cu bridging angles of 102.6(2) and 101.7(2)°. Thus, two bridging modes of the carboxylic groups coordinated to $Cu^{II}$ centers exist: $\mu\text{-}O, O'_{anti}\text{-}\mu\text{-}O_{syn}, O_{anti}$ (Scheme 2c, O7-C4-O11B and O6-C20-O5) and $\mu\text{-}O_{syn}, O'_{anti}$ (Scheme 2a, other carboxylic groups). The former carboxylic groups extend the coordination octahedrons into the infinite 1D supramolecular structure along the crystallographic [001] direction (Figure 4).

In analogy to the structure of **1**, a striking feature of **2** is that there is only one encapsulated $Na^+$ ion in the center of each cation cage; however it forms electrovalent bonds with the surrounding eight oxygen atoms of the carboxylic pendants (Figure 5). These bond lengths range from 2.388(4) to 2.672(4) Å with an average value of 2.538 Å for Na1 (range from 2.468(5) to 2.635(4) Å with average value of 2.544 Å for Na2), the bond angles lie between 67.1(2) and 106.9(1)° for Na1 and between 66.4(1) and 106.2(1) for Na2. The coordination spheres of both $Na^+$ ions could be best described as distorted square prisms. Thus, considering the coordination to both $Cu^{II}$ and $Na^+$, the bridging modes of the carboxylic groups in **2** are $\mu\text{-}O_{Cu}, O'_{Na(syn),Cu(anti)}\text{-}\mu\text{-}O_{Cu(syn)}, O_{Cu(anti)}\text{-}\mu\text{-}O'_{Cu(anti)}, O'_{Na(syn)}$ (Scheme 2d, for O7-C40-O11B and O6-C20-O5) or $\mu\text{-}O_{Cu(anti)}, O'_{Cu(syn)}\text{-}\mu\text{-}O_{Cu(anti)}, O_{Na(syn)}$ (Scheme 2b, other carboxylic groups). The former bridging mode is quite rare and is the first case for the linkage of two kinds of metal ions.[12] The six crystallographically independent Cu···Na distances are almost equivalent (3.397(1)–3.582(1) Å) with a mean value of 3.480 Å, and the eight Cu-O-Na bridging angles are in the 94.3(2)–103.2(2)° range, with an average value of 98.5°. All the DACO rings in the ligands adopt the normal *boat–chair* configuration,[8] and are bent so that the central C–H methylene group of the boat form of the metalladiazacyclohexane ring shields the $Cu^{II}$ center chelated to it with H···Cu distances of 2.456, 2.417, 2.459, and 2.447 Å, and H-Cu-Cl angles of 176.7, 179.3, 175.7, and 178.6°, respectively. Thus, as interpreted in several of our previous publications,[8] the methylene hydrogen atom effectively blocks the sixth coordination position of $Cu^{II}$, giving rise to the observed pentacoordinate geometry.

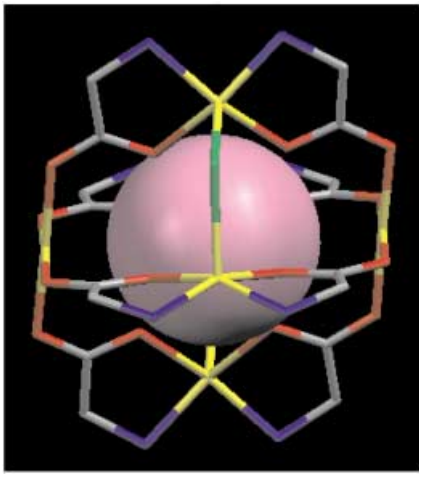

Figure 5. View of octahedral coordination cage in **2** (Cu: yellow; Cl: green; O: red; C: gray; N: blue; $Na^I$ template: purple).

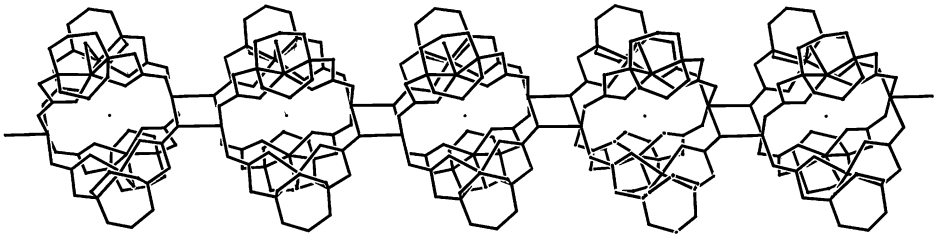

Figure 4. View of the 1D supramolecular chain of **2**. The dot in the center of each coordination cage represents the $Na^I$ ion.

**Roles of alkali-metal templates and ligand functionality in self-assemblies of compounds 1 and 2**: From the above descriptions, the appropriate choice of alkali-metal template ion ($Li^+$ or $Na^+$), together with a subtle change of the organic ligands,

are clearly critical in determining the supramolecular architectures of the resultant high-nuclear products. Recently, we demonstrated an interesting proton-controlled reversible interconversion between an *achiral* $Cu^{II}$ molecular square (pH≈2), and a 1D, spontaneously resolved, interpenetrated *chiral* double-chain with $Cu_4$ cavities (pH≈6), for a similar ligand $H_2L$ (see Scheme 1).[9b] However, for both ligands ($H_2L^1$ and $H_2L^2$) used in this study, only the simplex product **1** or **2** could be isolated at pH 4–5 following reaction with $Cu^{II}$. Although the three ligands have very similar frameworks, it is noteworthy that they form quite different resultant complexes upon metal complexation (with $[Cu(ClO_4)_2]$), which suggests that subtle variations of the backbone of the diazamesocyclic ligands or the pendant arms may result in quite different metal/organic coordination architectures. This further confirms that the diazamesocycles and their functionalized derivatives could be suitable for constructing metal/organic supramolecular entities with unusual structures and interesting properties. With regard to the self-assembly processes and the final structures of complexes **1** and **2**: first, the octahedral coordination cage observed in **2** exhibits a larger cavity than that of the coordinated tetrahedron in **1**; the $Na^+$ ion located in **2** was stabilized by electrovalent Na–O bonds (mean value: 2.541 Å) with a mean Na···Cu separation of 3.480 Å, and the $Li^+$ ion located in **1** has the average values for the Li–O and Li···Cu distances of 2.127 and 3.058 Å, respectively. A Cambridge Structural Database (CSD) search was performed for the related bond data: the average Na–O and Li–O bond lengths are 2.5 and 2.1 Å, respectively, and this is obviously consistent with the bond geometries found for the alkali-metal ions in different coordination polyhedra of compounds **1** and **2**. Second, although we tried several times using other alkali-metal ions as the template ($Na^+$ or $K^+$ ion for **1**, and $Li^+$ or $K^+$ ion for **2**), we found that solid products cannot be successfully separated from the final solution, although it is apparent that the complexation reaction occurred between the $Cu^{II}$ ion and the ligand in all these cases. This may be caused by the different ionic radii of these alkali-metal ions not matching the cavity of the tetrahedral or octahedral cage. It may also confirm that the template effect of the special alkali-metal ion plays a critical role in the formation of such supramolecular architectures. It should also be noted that, until now, most coordination polyhedra were constructed from $Pd^{II}$, $Pt^{II}$, or $Fe^{III}$, and that polynuclear architectures from $Cu^{II}$ are still quite rare.[1,13]

**Electronic and ESR spectra:** The UV/Vis spectra for complexes **1** and **2** in aqueous solution show a broad absorption maximum band centered at 619 and 646 nm, respectively. This spectral feature is typical of pentacoordinate $Cu^{II}$ complexes with (distorted) square-pyramidal geometry, which generally exhibit a band in the 550–660 nm range ($d_{xz}$, $d_{yz} \rightarrow d_{x^2-y^2}$).[14] In addition, the electronic spectra of both complexes display characteristic absorptions at 190–290 nm which are assigned to ligand transitions.

The X-band ESR spectra of both complexes were recorded in the polycrystalline powder state at different temperatures (room temperature, 77 K, and 4 K). For **1**, regardless of the temperature, the spectra do not show anisotropic features but only a sharp isotropic band centered at $g_{av} = 2.12$ (between 3000 and 3500 G, see Figure S1 in the Supporting Information), probably caused by exchange narrowing.[15] For **2**, at all temperatures, there is a typical pattern (see Figure S2 in the Supporting Information) of axial distortion for $Cu^{II}$ centers with $g_{\parallel} = 2.22$, $g_{\perp} = 2.06$ and $g_{av} = 2.11$, and there is no variation with the temperature. This pattern is typical for $Cu^{II}$ complexes with square-pyramidal geometry, with the unpaired electron mainly located in the $d_{x^2-y^2}$ orbital, which is consistent with the result of the crystal structure.

**Magnetic properties**: The magnetic behavior of **1** was measured on a SQUID susceptometer in the magnetic field range of 0.1 T from RT to 8 K and with 500 Gauss at 8–2 K to avoid any saturation phenomena at low temperature. The $\chi_M T$ value (magnetic susceptibility per 12 $Cu^{II}$ ions) is 4.81 $cm^3 mol^{-1} K^{-1}$ at 300 K, corresponding to twelve spin doublets. Then it increases inversely with the temperature (6.11 $cm^3 mol^{-1} K^{-1}$ at 5 K), and finally decreases down to a minimum value of 5.37 $cm^3 mol^{-1} K^{-1}$ at 2 K. This curve (Figure 6) suggests a ferromagnetic coupling with antiferromagnetic intramolecular/intermolecular interactions that are active at low temperature. The effect of the "molecular" $D$ parameter derived from the low-lying states of the $Cu_{12}$ entity could also explain this behavior (see below). The curve of $\chi_M$ is less significant: the value of $\chi_M$ at room temperature is 0.016 $cm^3 mol^{-1}$. The $\chi_M$ values are almost constant to ≈50 K and then increase rapidly until 2 K, attaining a value of 2.70 $cm^3 mol^{-1}$.

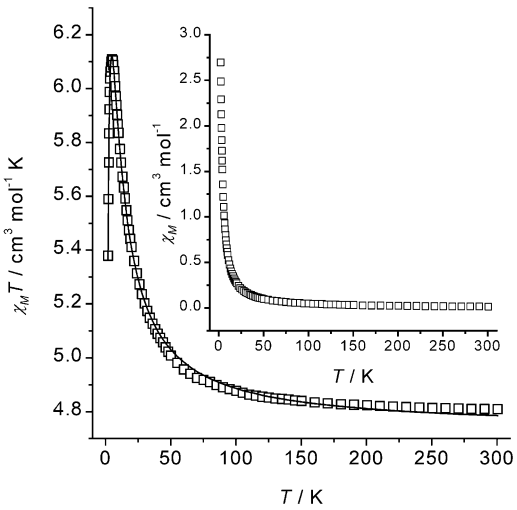


Figure 6. Plot of $\chi_M T$ and $\chi_M$ (inset) versus $T$ for twelve $Cu^{II}$ ions in **1**. The solid line represents the best fit for the $\chi_M T$ data obtained by the first method indicated in the text (with $J_1$, $J_2$, and $J_3$ considering the whole dodecanuclear entity). The fit has been made taking into account all the experimental points.

To interpret the magnetic behavior of **1**, it is convenient to schematize this dodecanuclear entity to clearly determine

  

which are the exchange pathways and the possible Hamiltonian. From the magnetic point of view, the $Cu^{II}$ ions are linked in a tetrahedral form with the corresponding $J$ parameters (Scheme 3). $J_1$ corresponds to the coupling between three *syn–anti* carboxylato bridges presenting basal–basal coordination (considering the square-pyramidal geometry of each $Cu^{II}$) between Cu4–Cu1, Cu4–Cu2, and Cu4–Cu3, respectively. $J_2$ corresponds to the coupling in three *syn–anti* carboxylato bridges between Cu1–Cu2, Cu2–Cu3, and Cu3–Cu1 in apical–basal coordination. Finally, $J_3$ corresponds to the coupling between three $Cu_4$ entities through the Cl central bridge in an apical–apical coordination. Thus, it corresponds to Cu4–Cu4A, Cu4–Cu4B, and Cu4A–Cu4B, respectively. Consequently, we have to interpret the magnetic behavior with a complicated dodecanuclear model that has three $J$ parameters with the following spin Hamiltonian [Eq. (1)].

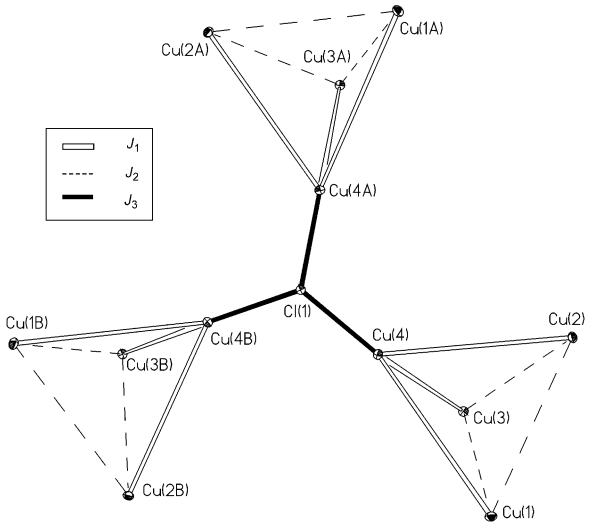


Scheme 3. Spin topology of **1**.

$$H = -J_1 \sum S_i S_j - J_2 \sum S_k S_l - J_3 \sum S_m S_n \quad (1)$$

The complete form is given in Equation (2).

$$\begin{aligned} H = & -J_1[(S_4S_1+S_4S_2+S_4S_3)+(S_{4A}S_{1A}+S_{4A}S_{2A}+S_{4A}S_{3A}) \\ & +(S_{4B}S_{1B}+S_{4B}S_{2B}+S_{4B}S_{3B})]-J_2[(S_1S_2+S_2S_3+S_3S_1) \\ & +(S_{1A}S_{2A}+S_{2A}S_{3A}+S_{3A}S_{1A})+(S_{1B}S_{2B}+S_{2B}S_{3B}+S_{3B}S_{1B})] \\ & -J_3(S_4S_{4A}+S_{4A}S_{4B}+S_{4B}S_4) \end{aligned} \quad (2)$$

A Hamiltonian with these three repeated $J$ parameters (along with the identical $g$ value) can not be solved by Kambe's method.[16] Thus, the fit was made by a full-diagonalization matrix method with the irreducible tensor operator formalism (ITO) calculated with the Clumag program,[17] leading to $J_1 = 6.4\ cm^{-1}$, $J_2 = 0.87\ cm^{-1}$, $J_3 = -3.5\ cm^{-1}$, $g = 2.10$, and $R = 5.5\times10^{-6}$. This could be a possible correlation between the $J$ values, being consistent with the structure: $J_1$ corresponds to *syn–anti* coordination in the out-of-plane conformation. This geometry always gives a small ferromagnetic coupling, as has been experimentally proved in many cases[18] and studied from a theoretical point of view.[19] Apparently, $J_2$ is the same case, but the smaller $J$ value is in accordance with the apical–basal coordination, which, logically, always gives smaller values than a basal–basal conformation. Finally, the apical–apical coupling through the $Cl^-$ ion ($J_3$) has to be small and antiferromagnetic. In this attempt, any possible interaction between the $Cu_{12}$ entities or the possible molecular $D$ parameter arising from the final ground state ($S = 6$) are impossible to consider.

The corresponding energy-level diagram has been derived from the Clumag fit (Figure 7 A). As can be clearly seen from this diagram, the "absolute" ground state would be $S = 0$ ($E = -18.1$ eV), which is practically degenerate with the states $S = 1$ ($E = -18.0$ eV), $S = 2$ ($E = -17.7$ eV), or $S = 3$ ($E = -17.4$ eV). Therefore, there is a mixture in the observed ground state in the magnetization curve measured at 2 K. This order of the states is mainly ascribed to

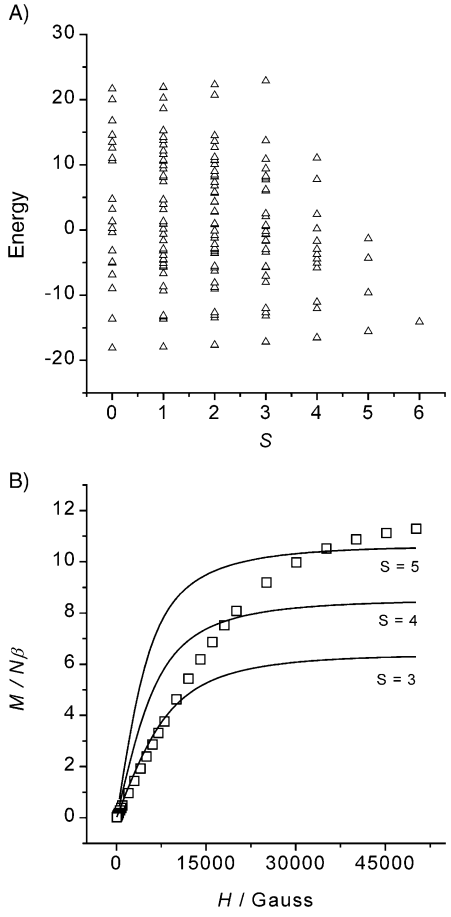


Figure 7. A) Plot of the energy of the spin states, calculated with the Clumag program (see text). Many of the energies are degenerate. B) Plot of the reduced magnetization curve at 2 K (□), compared with hypothetical Brillouin laws for $S = 5$, 4, 3, to show that the experimental magnetization does not follow the Brillouin equation.

the $J_3$ value, which is antiferromagnetic and almost of the same order of magnitude as the predominant $J_1$ ferromagnetic coupling. If $J_3$ was very slightly ferromagnetic, the ground state would be $S = 6$, as calculated with the same values of $J_1$ and $J_2$. For this reason, the reduced molar magnetization ($M/N\beta$) at 2 K does not follow the Brillouin formula for $S = 5$, 4, or 3 ground states (Figure 7B) at all. This important deviation from the Brillouin law can be caused either by antiferromagnetic coupling ($J_3$) or by the presence of some small "molecular" $D$ parameter for the $S \neq 0$ low-lying states. These states derive from $Cu^{II}$ ions, which do not have single-ion zero-field splitting. Gatteschi et al. have studied the ESR of several $Cu_4$ complexes by adding to the Zeeman term, the $B_4(O_4^0+5O_4^4)$ fourth-order cubic fine-structure operators ($B_4 = 0.0044\ cm^{-1}$).[20] This gives very small $|D|$ parameters, such as 0.04–0.09 $cm^{-1}$. Even with these small $|D|$ values, the ESR spectra shown by Gatteschi and co-workers are rather complicated and do not correspond in any way to the simple spectrum obtained for complex **1**. This feature seems to indicate that the $|D|$ parameter in complex **1** must be close to 0.

A simulation was carried out with the general procedure developed by Clemente et al. (MAGPACK program)[21] assuming an isotropic exchange for $D_{Cu4}$ ($S = 2$). Good mathematical results were obtained with the following parameters: $J_1 = 6.5 \pm 0.2\ cm^{-1}$; $J_2 = 0.1 \pm 0.02\ cm^{-1}$; $D_{Cu4} = 4.5 \pm 0.2\ cm^{-1}$, $g = 2.10$. These values were used to simulate the magnetization curve to compare them with the experimental values (now for four Cu ions). The best simulation is obtained with a low $D$ value, $\approx 1.7\ cm^{-1}$ (see Figure S3 in the Supporting Information). Both calculated $D$ values (from susceptibility and magnetization measurements) are too great for a polynuclear complex of $Cu^{II}$. Therefore, we can deduce that these $D$ values are probably theoretical ones, without chemical sense. The susceptibility and magnetization data must be interpreted by the presence of the antiferromagnetic $J_3$ parameter. The ESR spectra seem to indicate that $D_{Cu12}$ is zero or very close to zero.

Finally, as a complement of the first approach, we considered each $Cu_4$ entity, by changing the $J_3$ parameter (first approach) by $J'$ (molecular-field approximation) according to the theory of intermolecular interactions stated by Kahn.[22] With this hypothesis, the magnetic susceptibility can be fitted to the equation given for four $S = {}^1/_2$ spins in a $C_{3v}$ geometry (only $J_1$ and $J_2$ parameters)[23] and introducing a new $J'$ intertetramer parameter into the equation. A reasonably good fit can be obtained with the following parameters: $J_1 = 7.22\ cm^{-1}$, $J_2 \approx 0\ cm^{-1}$, $J_3$ ($J'$) $= -0.16\ cm^{-1}$, $g = 2.10$ and $R = 1.0 \times 10^{-5}$. In all cases, we considered the typical TIP value: $60 \times 10^{-6}\ cm^3\,mol^{-1}$ for each isolated $Cu^{II}$ ion.[22]

As a final conclusion for complex **1**, the susceptibility and magnetization curves can be explained by the presence of the two phenomena: $J_3$ or $J'$ due to Cu-Cl-Cu bridges rather than a possible very small $D_{Cu12}$ (zero-field splitting of the $S \neq 0$ low-lying states). The values obtained considering the $Cu_{12}$ entity (the most realistic from the structural point of view) agree with the feature indicating the $J_1$ value is always the greatest (6–7 $cm^{-1}$), but $J_2$ is greater under the $Cu_{12}$ consideration (close to 1 $cm^{-1}$) than under the other two considerations (close to 0 $cm^{-1}$). In any case, we can conclude that $J_1$ is dominant and ferromagnetic, $J_2$ is small and ferromagnetic, and $J_3 = J'$ is small and antiferromagnetic.

Figure 8 shows the magnetic properties of **2** in the form of $\chi_M T$ versus $T$ plots ($\chi_M$ = the molar magnetic susceptibility for twelve $Cu^{II}$ ions, as indicated below for the model of fit).

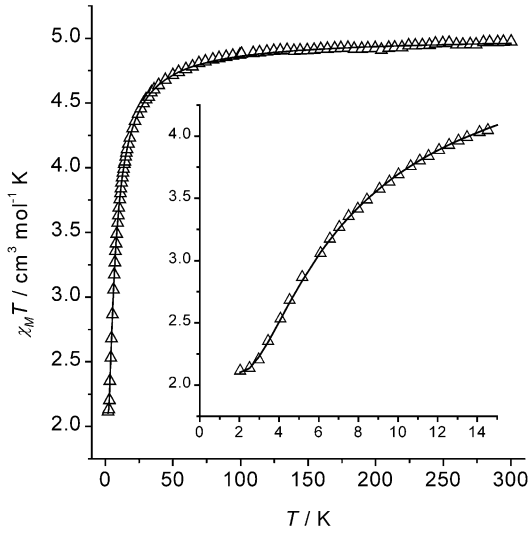


Figure 8. Temperature dependence of $\chi_M T$ (insert: low temperature region) for **2**. Experimental points △ and the solid line that is obtained by the fit indicated in the text.

The value of $\chi_M T$ at 300 K is 4.97 $cm^3\,mol^{-1}\,K^{-1}$ which is as expected for twelve magnetically quasi-isolated spin doublets. The $\chi_M T$ values smoothly decrease from room temperature to 50 K and then quickly decrease to 2.11 $cm^3\,mol^{-1}\,K^{-1}$ at 2 K. At very low temperatures, this decreasing tendency is stopped (Figure 8, insert). The global feature is characteristic of weak antiferromagnetic intramolecular interactions.

As shown in the crystallographic section, complex **2** consists of $Cu_6$ entities linked together by an asymmetric Cu(μ-O)$_2$Cu bridge to give a 1D system, in which two nonequivalent $Cu_6$ units exist. From the magnetic point of view, the structural differences are so small that we can consider to be negligible. Thus, two kinds of magnetic interactions must be considered to interpret the magnetic properties of **2**: intramolecular interactions (inside each $Cu_6$ unit) and intermolecular interactions (between adjacent $Cu_6$ units).

*Intramolecular interactions: a) syn–anti carboxylato interactions*: This pathway exists between Cu3-Cu1-Cu3-Cu1 and between Cu3-Cu2-Cu3-Cu2, which both share the Cu3 ions (between Cu4-Cu6-Cu4-Cu6 and between Cu4-Cu5-Cu4-Cu5 in another Cu6 unit, Scheme 4). Weak antiferromagnetic or ferromagnetic interactions were observed in the $Cu^{II}$ complexes bridged by carboxylato ligands in the *syn–anti* mode.[18b,d,24] The small overlap between the magnetic orbitals of the $Cu^{II}$ atoms through the *syn–anti* carboxylato

  

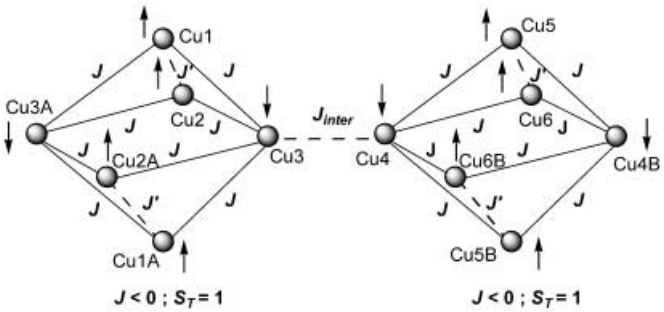


Scheme 4. Spin topology for **2** assuming three different *J* values.

bridge, for a Cu-O-C-O-Cu skeleton that is planar, accounts for the weak antiferromagnetic coupling observed. For example, in [(dien)Cu(μ-tp)Cu(dien)]($ClO_4$) (tp = terephthalate, dien = diethylenetriamine) $J = -3.66\ cm^{-1}$;[25a] and in [$Cu(NH_3)_2(CH_3COO)Br$] $J = -3.0\ cm^{-1}$.[25b] This overlap is significantly reduced for the cases in which the Cu-O-C-O-Cu skeleton deviates from planarity (out-of-phase exchange pathway, such as the $J_1$ interaction in **1**), thus reducing the antiferromagnetic contribution, and the ferromagnetic term becomes dominant.[18] In the case discussed here, the relative orientation of the metal-centered magnetic orbitals within the cluster is the planar conformation as shown in Scheme 5.

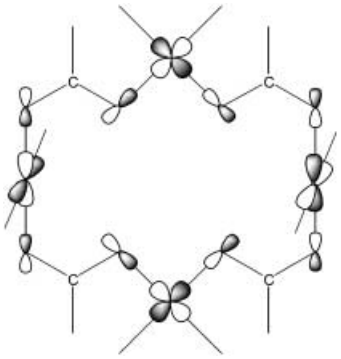

Scheme 5.

The magnetic orbitals at each copper atom are defined by the short equatorial bonds, and are of the $d_{x^2-y^2}$ type with some possible mixture of the $d_{z^2}$ character in the axial position. Thus it can be seen that the out-of-plane exchange pathway is minimum, and consequently, antiferromagnetic couplings would be predicted. Let us assume that according to the experimental magnetic values and this hypothesis, the coupling is antiferromagnetic. b) *Cu1-Cl2-Cu2 (and Cu5-Cl1-Cu6)*: The Cu1 and Cu2 (or Cu5 and Cu6) ions are linked by a chloro bridge, but with long apical Cu–Cl bond lengths (≈2.5 Å). This feature creates a net *J′* magnetic pathway. The unpaired electrons in these $Cu^{II}$ ions are mainly in the magnetic orbital $d_{x^2-y^2}$, thus the participation in the $d_{z^2}$ will be minimal. The pathway Cu1-Cl-Cu2 would be effective only if the $d_{z^2}$ is operative. Taking into account the structure and the geometry around the Cu atoms (together with the ESR spectra), this *J′* value must be very small (antiferromagnetic or ferromagnetic). Scheme 4 shows the resulting electron distribution and the $S_T$ value. According to this distribution (this is a new molecular ferrimagnetic situation), the final $S_T$ is not zero but one (two unpaired electrons). This feature explains why in the very low temperature region the $\chi_M T$ values tend to $1\ cm^3 mol^{-1} K^{-1}$ (corresponding to two correlated electrons) for a $Cu_6$ unit (Figure 8).

*Intermolecular interactions*: Finally, the intermolecular connection, $J_{inter}$ (Cu3-O7-O6-Cu4), must be considered. The Cu3 and Cu4 ions participate in the linkage of the $Cu_6$ entities to produce the 1D structure. The main bond lengths in the bridge are: Cu4–O6 = 2.353, O6–Cu3 = 1.997, Cu3–O7 = 2.327, and O7–Cu4 = 1.989 Å. There are, thus, two long and two short bond lengths. The unpaired electrons are mainly in the $d_{x^2-y^2}$ orbitals, directed through the Cu3–O6 and Cu4–O7 bonds. This apical–equatorial bond gives orthogonality (overlap zero) of the magnetic orbitals, hence the coupling must be zero or small ferromagnetic.

With these considerations, an attempt was made to fit the $\chi_M T$ data, assuming two ideal $Cu_6$ octahedra with parameters *J*, *J′*, and $J_{inter}$, local $S = {}^1/_2$ and $g = 2.11$ (according to the ESR measurements), and using the Clumag program[17] with the Hamiltonian $H = -J_i \Sigma S_i S_j$. The best-fit parameters are $J = -3.13\ cm^{-1}$, $J' = -0.019\ cm^{-1}$, $J_{inter} = 0.010\ cm^{-1}$, and $R = 1.3 \times 10^{-6}$ (*R* is the agreement factor defined as $\Sigma i[(\chi_m T)_{obs} - (\chi_m T)_{calcd}]^2 / \Sigma i[(\chi_m T)_{obs}]^2$, TIP was assumed to be $60 \times 10^{-6}\ cm^3 mol^{-1}$ per Cu atom). These values indicate that the coupling between the $Cu^{II}$ centers is slightly antiferromagnetic and of the same order as that found for similar planar *syn–anti* carboxylato-bridged metal complexes. The *J′* and $J_{inter}$ values are mathematically correlated and almost zero. The *R* value does not significantly change, assuming *J′* or $J_{inter} = 0$. For example, making a fit with only a $Cu_6$ entity ($J_{inter} = 0$), the best-fit parameters are $J = -3.13\ cm^{-1}$ and $J' = -0.018\ cm^{-1}$. The reduced molar magnetization ($M/N\beta$) per Cu ion tends to 0.4 electrons instead to 1 electron at 2 K when the field tends to 5 T. This feature agrees with the antiferromagnetic coupling within the six $Cu^{II}$ ions (see Figure S4 in the Supporting Information).

## Conclusion

In conclusion, the present work demonstrates successful examples of the self-assembly of two unique supramolecular aggregates with tetrahedral or octahedral coordination polyhedra that uses an alkali-metal ion ($Li^+$ or $Na^+$) as a template and well-designed carboxylic-functionalized diazamesocyclic ligands. This also provides additional proof of the extraordinary versatility and innumerable bridging possibilities of carboxylic ligands and diazamesocycles and, consequently, opens further perspectives for the experimentalists. Finally, the procedures described here could be generally applicable for analogous organic ligands and different metal ions (or mixed-metal system such as Cu–Ln) in constructing other magnetic clusters with unprecedented spin topologies and desirable properties. This is currently being investigated in our laboratory.

## Experimental Section

**Materials and general methods**: With the exception of 1,5-diazacyclooctane (DACO), which was synthesized according to a literature procedure,[26] all of the starting materials and solvents were purchased and used as received. FT-IR spectra (KBr pellets) were recorded on a FT-IR 170SX (Nicolet) spectrometer and electronic absorption spectra on a Hitachi UV-3010 spectrometer. Carbon, hydrogen, and nitrogen analyses were performed on a Perkin-Elmer 240C analyzer. $^1$H NMR spectra were recorded on a Bruker AC-P 400 spectrometer (400 MHz) at 25 °C with tetramethylsilane as the internal reference. ESR spectra were recorded on powder samples at the X-band frequency with a Bruker 300E automatic spectrometer at temperatures between 4 and 300 K.

**Magnetic studies**: The variable-temperature (2-300 K) magnetic susceptibilities were measured in "Servei de Magnetoquímica (Universitat de Barcelona)" on polycrystalline samples (≈30 mg) with a Quantum Design MPMS SQUID susceptometer operating with a magnetic field of 0.1 T. The diamagnetic corrections were evaluated from Pascal's constants for all the constituent atoms. Magnetization measurements were carried out at low temperature (2 K) in the 0–5 T range.

**Synthesis of the ligands *N,N′*-Bis(3-propionyloxy)-1,4-diazacycloheptane hydrochloride hydrate ($H_2L^1$·HCl·$H_2O$)**: 3-Bromopropionic acid (7.45 g, 48.7 mmol) was added with vigorous stirring under reflux to a solution of DACH (2.14 g, 21.4 mmol) in $C_2H_5OH$ (150 mL). Suitable portions of solid LiOH were added to keep the pH value of the mixture at ≈9 during this procedure. After stirring for 24 h, the mixture was filtered. $H_2L^1$·HCl·$H_2O$ was obtained as a white crystalline solid upon acidification (adjusted with 6 M HCl solution) and was recrystallized from $H_2O$/$CH_3OH$ in 80% yield (5.1 g, based on DACH). $^1$H NMR (400 MHz, $D_2O$): $\delta$ = 2.17–2.19 (m, 2H), 2.62–2.67 (t, $J$ = 8.8 Hz, 4H), 3.34–3.39 (t, $J$ = 8.8 Hz, 4H), 3.43–3.46 (t, $J$ = 7.2 Hz, 4H), 3.676 ppm (s, 4H); FT-IR (KBr pellet): $\tilde{\nu}$ = 3430 b, 2963 m, 2619 m, 1968 w, 1720 vs, 1586 s, 1400 vs, 1334 m, 1231 s, 1107 m, 1038 w, 996 m, 938 w, 848 w, 810 w, 781 w, 732 m cm$^{-1}$; elemental analysis calcd (%) for $H_2L^1$·HCl·$H_2O$ ($C_{11}H_{23}ClN_2O_5$): C 44.22, H 7.76, N 9.38; found: C 44.20, H 7.98, N 9.28.

**1,5-Diazacyclooctane-*N,N′*-diacetate acid dihydrochloride ($H_2L^2$·2HCl)**: A solution of DACO·2HBr (2.31 g, 8.37 mmol) and LiOH (1.96 g, 44.4 mmol) in $C_2H_5OH$ (30 mL) was stirred for 4 h at room temperature. A solution of 2-chloroacetic acid (1.72 g, 18.3 mmol) in $C_2H_5OH$ (30 mL) was added dropwise over 3 h to the stirred solution. The mixture was heated at reflux for 20 h at pH≈9. The ligand $H_2L^2$·2HCl was obtained as a white solid after acidification (pH≈2, adjusted with 6 M HCl solution) and recrystallization from $H_2O$/$CH_3OH$ in 80% yield (2.1 g, based on DACO·2HBr). $^1$H NMR (400 MHz, $D_2O$): 2.34–2.42 (m, 4H), 3.53 (t, $J$ = 6.0 Hz, 8H), 4.01 ppm (s, 4H); FT-IR (KBr pellet): $\tilde{\nu}$ = 3416 b, 2966 m, 2931 w, 1747 vs, 1478 m, 1461 m, 1427 s, 1378 s, 1354 m, 1223 vs, 1200 s, 1107 s, 1091 m, 1049 m, 851 m, 833 m, 794 w cm$^{-1}$; elemental analysis calcd (%) for $H_2L^2$·2HCl ($C_{10}H_{20}Cl_2N_2O_4$): C 39.62, H 6.65, N 9.24; found: C 39.47, H 6.98, N 9.03.

**Preparation of the $Cu^{II}$ complexes {($\mu_3$-Cl)[Li⊂$Cu_4$($\mu$-$L^1$)$_3$]$_3$}($ClO_4$)$_8$($H_2O$)$_{4.5}$ (1)**: [Cu($ClO_4$)$_2$]·6$H_2O$ (167 mg, 0.45 mmol) and $H_2L^1$·HCl·$H_2O$ (99 mg, 0.33 mmol) were allowed to react in MeOH/$H_2O$ (20 mL:5 mL) at room temperature. The pH value of this solution was adjusted to ≈4 with dilute aqueous LiOH solution. The reaction mixture was filtered and left in a vacuum. Dark blue crystals were obtained after two weeks by slow evaporation of the solvent in ≈50% yield (72 mg). IR (KBr pellet): $\tilde{\nu}$ = 3431 b, 2957 w, 2872 w, 1608 vs, 1577 vs, 1485 m, 1456 s, 1432 s, 1406 vs, 1336 m, 1299 w, 1259 w, 1217 w, 1096 vs, 1021 vs, 936 w, 883 m, 853 w, 750 m, 712 w, 624 s cm$^{-1}$; elemental analysis calcd (%) for **1** ($C_{99}H_{177}Cl_9Cu_{12}N_{18}Li_3O_{75.5}$): C 30.26, H 4.54, N 4.99; found: C 30.19, H 4.89, N 4.67.

**{[$Na_2$⊂$Cu_{12}$($\mu$-$L^2$)$_8$($\mu$-Cl)$_4$]($ClO_4$)$_8$($H_2O$)$_{10}$($H_3O^+$)$_2$}$_\infty$ (2)**: [Cu($ClO_4$)$_2$]·6$H_2O$ (113 mg, 0.3 mmol) and $H_2L^2$·2HCl (60 mg, 0.2 mmol) were allowed to react in MeOH/$H_2O$ (15 mL: 5 mL) at room temperature. The pH value of this solution was adjusted to ≈4–5 with dilute aqueous NaOH solution. The reaction mixture was filtered and left in a vacuum. Dark blue crystals were obtained after one month by slow evaporation of the solvent in ≈55% yield (52 mg). IR (KBr pellet): $\tilde{\nu}$ = 3450 b, 2940 w, 1647 vs, 1612 vs, 1448 m, 1418 s, 1381 m, 1332 m, 1254 m, 1227 w, 1142 vs, 1114 vs, 1089 vs, 1046 m, 1000 m, 974 m, 956 w, 940 w, 844 w, 823 w, 782 w, 724 m, 636 s, 627 s cm$^{-1}$; elemental analysis calcd (%) for **2** ($C_{80}H_{154}Cl_{12}Cu_{12}N_{16}Na_2O_{76}$): C 25.35, H 4.10, N 5.91; found: C 25.69, H 4.22, N 5.77.

**CAUTION!** Perchlorate complexes of metal ions in the presence of organic ligands are potentially explosive. Only a small amount of material should be handled with care.

**X-ray data collection and structure determinations**: X-ray single-crystal diffraction data for complexes **1** and **2** were collected on a Bruker Smart 1000 CCD area-detector diffractometer at 293(2) K with $Mo_{K\alpha}$ radiation ($\lambda$ = 0.71073 Å) in the $\omega$ scan mode. The program SAINT[27] was used to integrate the diffraction profiles. All the structures were solved by direct methods with the SHELXS program of the SHELXTL package and refined by full-matrix least-squares methods with SHELXL (semiempirical absorption corrections were applied with the SADABS program).[28] $Cu^{II}$ atoms in each complex were located from the $E$ maps and the other non-hydrogen atoms were located in successive difference-Fourier syntheses and refined with anisotropic thermal parameters on $F^2$. The hydrogen atoms of the ligands were generated theoretically onto the specific atoms and refined isotropically with fixed thermal factors. Further details for structural analysis are summarized in Table 3.

CCDC-204894 and CCDC-213111 contain the supplementary crystallographic data for this paper. These data can be obtained free of charge via www.ccdc.cam.ac.uk/conts/retrieving.html (or from the Cambridge Crystallographic Data Centre, 12 Union Road, Cambridge CB2 1EZ, UK; fax: (+44) 1223-336033; or deposit@ccdc.cam.uk).

Table 3. Crystal data and structure refinement parameters for complexes **1** and **2**.

| | **1** | **2** |
|---|---|---|
| chemical formula | $C_{99}H_{177}Cl_9Cu_{12}N_{18}Li_3O_{75.5}$ | $C_{80}H_{154}Cl_{12}Cu_{12}N_{16}Na_2O_{76}$ |
| $M_r$ | 3929.94 | 3790.05 |
| crystal system | trigonal | triclinic |
| space group | $R\bar{3}c$ | $P\bar{1}$ |
| $a$ [Å] | 20.866(3) | 13.632(4) |
| $b$ [Å] | 20.866(3) | 14.754(4) |
| $c$ [Å] | 126.26(4) | 19.517(6) |
| $\alpha$ [°] | 90 | 99.836(6) |
| $\beta$ [°] | 90 | 95.793(5) |
| $\gamma$ [°] | 120 | 116.124(5) |
| $V$ [Å$^3$] | 47607(18) | 3403(2) |
| $Z$ | 12 | 1 |
| $\rho_{calcd}$ [g cm$^{-3}$] | 1.645 | 1.849 |
| $F$(000) | 24132 | 1928 |
| $\mu$ [cm$^{-1}$] | 18.23 | 21.84 |
| measured reflections | 62616 | 17692 |
| independent reflections | 9255 | 13155 |
| $R_{int}$ | 0.1491 | 0.0429 |
| $S$ | 0.998 | 0.999 |
| $R^{[a]}$ | 0.0767 | 0.0620 |
| $R_w^{[b]}$ | 0.1880 | 0.1142 |

[a] $R = \Sigma||F_o|-|F_c||/\Sigma|F_o|$. [b] $R_w = [\Sigma[w(F_o^2-F_c^2)^2]/\sigma w(F_o^2)^2]^{1/2}$.

## Acknowledgement

This work was financially supported by the Outstanding Youth Foundation of NSFC (No. 20225101) and the Spanish government (Grant B-QU2000-0791).

  

[1] Recent reviews: a) M. Fujita, *Chem. Soc. Rev.* **1998**, *27*, 417–425; b) R. E. P. Winpenny, *Chem. Soc. Rev.* **1998**, *27*, 447–452; c) D. L. Caulder, K. N. Raymond, *Acc. Chem. Res.* **1999**, *32*, 975–982; d) R. W. Saalfrank, E. Uller, B. Demleitner, I. Bernt, *Struct. Bonding (Berlin)* **2000**, *96*, 149–175; e) S. Leininger, B. Olenyuk, P. J. Stang, *Chem. Rev.* **2000**, *100*, 853–908; f) G. F. Swiegers, T. J. Malefetse, *Chem. Eur. J.* **2001**, *7*, 3636–3643; g) B. J. Holliday, C. A. Mirkin, *Angew. Chem.* **2001**, *113*, 2076–2098; *Angew. Chem. Int. Ed.* **2001**, *40*, 2022–2043; h) S. R. Seidel, P. J. Stang, *Acc. Chem. Res.* **2002**, *35*, 972–983.

[2] Selected examples: a) R. Sessoli, H.-L. Tsai, A. R. Schake, S. Wang, J. B. Vincent, K. Folting, D. Gatteschi, G. Christou, D. N. Hendrickson, *J. Am. Chem. Soc.* **1993**, *115*, 1804–1816; b) C. Sangregorio, T. Ohm, C. Paulsen, R. Sessoli, D. Gatteschi, *Phys. Rev. Lett.* **1997**, *78*, 4645–4648; c) Z. Sun, C. M. Grant, S. L. Castro, D. N. Hendrickson, G. Christou, *Chem. Commun.* **1998**, 721–722; d) A. L. Barra, A. Caneschi, A. Cornia, F. F. de Biani, D. Gatteschi, C. Sangregorio, R. Sessoli, L. Sorace, *J. Am. Chem. Soc.* **1999**, *121*, 5302–5303.

[3] Selected examples: a) J. S. Fleming, K. L. V. Mann, C.-A. Carraz, E. Psillakis, J. C. Jeffery, J. A. McCleverty, M. D. Ward, *Angew. Chem.* **1998**, *110*, 1315–1317; *Angew. Chem. Int. Ed.* **1998**, *37*, 1279–1281; b) R. W. Saalfrank, N. Low, B. Demleitner, D. Stalke, M. Teichert, *Chem. Eur. J.* **1998**, *4*, 1305–1311; c) M. Ziegler, J. J. Miranda, U. N. Andersen, D. W. Johnson, J. A. Leary, K. N. Raymond, *Angew. Chem.* **2001**, *113*, 755–758; *Angew. Chem. Int. Ed.* **2001**, *40*, 733–736; d) Z. R. Bell, J. C. Jeffery, J. A. McCleverty, M. D. Ward, *Angew. Chem.* **2002**, *114*, 2625–2628; *Angew. Chem. Int. Ed.* **2002**, *41*, 2515–2518.

[4] Selected examples: a) M. I. Khan, J. Zubieta, *Prog. Inorg. Chem.* **1995**, *43*, 1–149, and references therein; b) M. G. Walawalker, H. W. Roesky, R. Murugavel, *Acc. Chem. Res.* **1999**, *32*, 117–126, and references therein; c) V. Chandrasekhar, S. Kingsley, *Angew. Chem.* **2000**, *112*, 2410-2412; *Angew. Chem. Int. Ed.* **2000**, *39*, 2320–2322; d) W. F. Ruettinger, G. C. Dismukes, *Inorg. Chem.* **2000**, *39*, 1021–1027; e) E. K. Brechin, R. A. Coxall, A. Parkin, S. Parsons, P. A. Tasker, R. E. P. Winpenny, *Angew. Chem.* **2001**, *113*, 2772–2775; *Angew. Chem. Int. Ed.* **2001**, *40*, 2700–2703.

[5] Selected examples: a) S. Mann, G. Huttner, L. Zsolnai, K. Heinze, *Angew. Chem.* **1996**, *108*, 2983–2984; *Angew. Chem. Int. Ed.* **1996**, *35*, 2808–2809; b) R. Vilar, D. M. P. Mingos, A. J. P. White, D. J. Williams, *Angew. Chem.* **1998**, *110*, 1323–1326; *Angew. Chem. Int. Ed.* **1998**, *37*, 1258–1261; c) K. K. Klausmeyer, S. R. Wilson, T. B. Rauchfuss, *J. Am. Chem. Soc.* **1999**, *121*, 2705–2711.

[6] W. Wernsdorfer, N. Aliaga-Alcalde, D. N. Hendrickson, G. Christou, *Nature* **2002**, *416*, 406–409, and references therein.

[7] a) S. M. Contakes, T. B. Rauchfuss, *Chem. Commun.* **2001**, 553–554; b) R. W. Saalfrank, R. Burak, A. Breit, D. Stalke, R. Herbst-Irmer, J. Daub, M. Porsch, E. Bill, M. Müther, A. X. Trautwein, *Angew. Chem.* **1994**, *106*, 1697–1699; *Angew. Chem. Int. Ed. Engl.* **1994**, *33*, 1621–1623; c) R. W. Saalfrank, I. Bernt, E. Uller, F. Hampel, *Angew. Chem.* **1997**, *109*, 2596–2599; *Angew. Chem. Int. Ed. Engl.* **1997**, *36*, 2482–2485; d) D. L. Caulder, R. E. Powers, T. N. Parac, K. N. Raymond, *Angew. Chem.* **1998**, *110*, 1940–1943; *Angew. Chem. Int. Ed.* **1998**, *37*, 1840–1843; e) A. Cornia, M. Affronte, A. G. M. Jansen, G. L. Abbati, D. Gatteschi, *Angew. Chem.* **1999**, *111*, 2409–2411; *Angew. Chem. Int. Ed.* **1999**, *38*, 2264–2266; f) L. Y. Wang, S. Igarashi, Y. Yukawa, Y. Hoshino, O. Roubeau, G. Aromi, R. E. P. Winpenny, *J. Chem. Soc. Dalton Trans.* **2003**, 2318–2324.

[8] Selected examples: a) X. H. Bu, M. Du, Z. L. Shang, R. H. Zhang, D. Z. Liao, M. Shionoya, T. Clifford, *Inorg. Chem.* **2000**, *39*, 4190–4199; b) X. H. Bu, M. Du, L. Zhang, D. Z. Liao, J. K. Tang, R. H. Zhang, M. Shionoya, *J. Chem. Soc. Dalton Trans.* **2001**, 593–598; c) X. H. Bu, M. Du, L. Zhang, Z. L. Shang, R. H. Zhang, M. Shionoya, *J. Chem. Soc. Dalton Trans.* **2001**, 729–735; d) X. H. Bu, M. Du, Z. L. Shang, L. Zhang, Q. H. Zhao, R. H. Zhang, M. Shionoya, *Eur. J. Inorg. Chem.* **2001**, 1551–1558; e) M. Du, Y. M. Guo, X. H. Bu, J. Ribas, M. Monfort, *New J. Chem.* **2002**, *26*, 645–650; f) M. Du, Y. M. Guo, X. H. Bu, J. Ribas, M. Monfort, *New J. Chem.* **2002**, *26* ,939–945.

[9] a) M. Du, X. H. Bu, Y. M. Guo, L. Zhang, D. Z. Liao, J. Ribas, *Chem. Commun.* **2002**, 1478–1479; b) M. Du, X. H. Bu, Y. M. Guo, J. Ribas, C. Diaz, *Chem. Commun.* **2002**, 2550–2551.

[10] C. A. Grapperhaus, M. Y. Darensbourg, *Acc. Chem. Res.* **1998**, *31*, 451–459, and references therein.

[11] A. W. Addison, T. N. Rao, J. Reedijk, J. V. Rijn, G. C. Verschoor, *J. Chem. Soc. Dalton Trans.* **1984**, 1349–1356.

[12] a) K.-C. Yang, C.-C. Chang, C.-S. Yeh, G.-H. Lee, S.-M. Peng, *Organometallics* **2001**, *20*, 126–137; b) M. T. Caudle, J. B. Benedict, C. K. Mobley, N. A. Straessler, T. L. Groy, *Inorg. Chem.* **2002**, *41*, 3183–3190.

[13] a) P. J. Stang, B. Olenyuk, *Acc. Chem. Res.* **1997**, *30*, 502–518; b) S. Hiraoka, M. Fujita, *J. Am. Chem. Soc.* **1999**, *121*, 10239–10240.

[14] G. A. McLachlan, G. D. Fallon, R. L. Martin, L. Spiccia, *Inorg. Chem.* **1995**, *34*, 254–261.

[15] C. R. Lucas, S. Liu, L. K. Thompson, *Inorg. Chem.* **1990**, *29*, 85–88.

[16] K. Kambe, *J. Phys. Soc. Japan* **1950**, *5*, 48–51.

[17] The series of calculations were made with the computer program Clumag, which uses the irreducible tensor operator (ITO) formalism: D. Gatteschi, L. Pardi, *Gazz. Chim. Ital.* **1993**, *123*, 231–240. We thank Profs. Dante Gatteschi (University of Firenze, Italy) and Vassilis Tangoulis (University of Patras, Greece) for kindly supplying this program.

[18] a) D. K. Towle, S. K. Hoffmann, W. E. Hatfield, P. Singh, P. Chaudhuri, *Inorg. Chem.* **1988**, *27*, 394–399; b) E. Colacio, J. P. Costes, R. Kivekas, J. P. Laurent, J. Ruiz, *Inorg. Chem.* **1990**, *29*, 4240–4246; c) E. Colacio, J. M. Domínguez-Vera, J. P. Costes, R. Kivekas, J. P. Laurent, J. Ruiz, M. Sundberg, *Inorg. Chem.* **1992**, *31*, 774–778; d) C. Ruiz-Pérez. J. Sanchis, M. Hernández-Molina, F. Lloret, M. Julve, *Inorg. Chem.* **2000**, *39*, 1363–1370, and references therein.

[19] A. Rodríguez-Fortea, P. Alemany, S. Alvarez, E. Ruiz, *Chem. Eur. J.* **2001**, *7*, 627–637.

[20] A. Bencini, D. Gatteschi, *EPR of Echange Coupled Systems*, Springer, Berlin, **1990**.

[21] a) J. J. Borrás-Almenar, J. M. Clemente-Juan, E. Coronado, B. S. Tsukerblat, *Inorg. Chem.* **1999**, *38*, 6081–6088; b) J. J. Borrás-Almenar, J. M. Clemente-Juan, E. Coronado, B. S. Tsukerblat, *J. Comput. Chem.* **2001**, *22*, 985–991.

[22] O. Kahn, *Molecular Magnetism*, VCH Publishers, New York, **1993**.

[23] R. W. Jotham, S. F. A. Kettle, *Inorg. Chim. Acta* **1970**, *4*, 145–149.

[24] a) K. K. Nanda, A. W. Addison, E. Sinn, L. K. Thompson, *Inorg. Chem.* **1996**, *35*, 5966–5967; b) C. Ruiz-Pérez, M. Hernández-Molina, P. Lorenzo-Luis, F. Lloret, J. Cano, M. Julve, *Inorg. Chem.* **2000**, *39*, 3845–3852.

[25] a) E. Bakalbassis, C. Tsipis, A. Bozopoulos, W. Dreissing, H. Hartl, J. Mrozinski, *Inorg. Chim. Acta* **1991**, *186*, 113–118; b) R. Carlin, K. Kopinga, O. Kahn, M. Verdaguer, *Inorg. Chem.* **1986**, *25*, 1786–1789.

[26] a) E. L. Buhle, A. M. Moore, F. Y. Wiselogle, *J. Am. Chem. Soc.* **1943**, *65*, 29–32; b) J. H. Billman, L. C. Dorman, *J. Org. Chem.* **1962**, *27*, 2419–2422.

[27] Bruker AXS, *SAINT Software Reference Manual*, Madison, WI, **1998**.

[28] G. M. Sheldrick, SHELXTL NT Version 5.1. Program for Solution and Refinement of Crystal Structures, University of Göttingen (Germany), **1997**.

Received: July 3, 2003
Revised: October 23, 2003 [F5300]